ORIGINAL ARTICLE

Journal of Anatomy

ANATOMICAL SOCIETY WILEY

Fin systems comparative anatomy in model Batoidea *Raja asterias* and *Torpedo marmorata*: Insights and relatioships between musculo-skeletal layout, locomotion and morphology

Ugo E. Pazzaglia[1,2] | Marcella Reguzzoni[2] | Renata Manconi[3] | Luca Lanteri[4] |
Guido Zarattini[1] | Piero A. Zecca[2] | Mario Raspanti[2]

[1]DSMC, University of Brescia, Brescia, Italy

[2]DMC, University of Insubria, Varese, Italy

[3]DVM (Zoology Lab), University of Sassari, Sassari, Italy

[4]DISTAV, University of Genova, Genova, Italy

Correspondence
Ugo E. Pazzaglia and Marcella Reguzzoni, DMC, University of Insubria, Varese, Italy.
Email: u.e.pazzaglia@gmail.com and marcella.reguzzoni@uninsubria.it

Abstract

The macroscopic and microscopic morphology of the appendicular skeleton was studied in the two species *Raja asterias* (order Rajiformes) and *Torpedo marmorata* (Order Torpediniformes), comparing the organization and structural layout of pectoral, pelvic, and tail fin systems. The shape, surface area and portance of the *T. marmorata* pectoral fin system (hydrodynamic lift) were conditioned by the presence of the two electric organs in the disk central part, which reduced the pectoral fin surface area, suggesting a lower efficiency of the "flapping effectors" than those of *R. asterias*. Otherwise, radials' rays alignment, morphology and calcification pattern showed in both species the same structural layout characterized in the fin medial zone by stiffly paired columns of calcified tiles in the perpendicular plane to the flat batoid body, then revolving and in the horizontal plane to continue as separate mono-columnar rays in the fin lateral zone with a morphology suggesting fin stiffness variance between medial/lateral zone. Pelvic fins morphology was alike in the two species, however with different calcified tiles patterns of the 1st compound radial and pterygia in respect to the fin-rays articulating perpendicularly to the latter, whose tile rows lay-out was also different from that of the pectoral fins radials. The *T. marmorata* tail-caudal fin showed a muscular and connective scaffold capable of a significant oscillatory forward thrust. On the contrary, the *R. asterias* dorsal tail fins were stiffened by a scaffold of radials-like calcified segments. Histomorphology, heat-deproteination technique and morphometry provided new data on the wing-fins structural layout which can be correlated to the mechanics of the Batoid swimming behavior and suggested a cartilage-calcification process combining interstitial cartilage growth (as that of all vertebrates anlagen) and a mineral deposition with accretion of individual centers (the tiles). The resulting layout showed scattered zones of un-mineralized matrix within the calcified mass and a less compact texture of the matrix calcified fibers suggesting a possible way of fluid diffusion throughout the mineralized tissue. These observations could explain the survival of the embedded chondrocytes in absence of a canalicular system as that of the cortical bone.

1 | INTRODUCTION

The super-order of Batoids (Rajiomorphii) is delineated among the cartilaginous fishes by the common morpho-trait of flattened and large, pectoral fins (wings) fused to the head and a posterior system of pelvic and tail fins. The pectoral fins show a stratified layout of dorsal and ventral muscles, calcified segments (pterygia and radials), a high number of joints with variable range of movement and a large, widespread membrane dividing the dorsal from the ventral muscles (Pazzaglia et al., 2022b). They have developed together with the pelvic and tail fins as an integrated system of variable flexural stiffness and strength capable of producing species-specific locomotion patterns in the water column (Compagno, 1973, 1977). The swimming styles of this super-order have been distinguished in "Mobuliform", characterized by flapping of the pectoral fins (in pelagic Myliobatiformes species as manta rays) and "Rajiform" with an undulating movement of the pectoral fins distal part which forms multiple waves present in the fin at the same time (Rosenberger, 2001; Taft, 2011). The variable morpho-type (size, shape, number of rays and morpho of the calcified elements) of pectoral, pelvic and tail fins are the anatomical traits currently used to distinguish the Rajiomorphii species, further classified in Rajiformes, Torpediniformes and Miliobatiformes orders (Compagno, 1999; McEachran & Dunn, 1998; Regan, 1906; Serena et al., 2010).

The macroscopic and microscopic morphology of the appendicular skeleton allows to distinguish two calcification types: the first with mineralized units of polygonal shape known as "tesserae" developing on the skeletal segments surface of the most bulky skeletal segments (compound radials, pterygia and girdles) with the related calcification pattern termed as "crustal"; the second with aligned cylindrical units or "calcified cylindrical tiles" and the related pattern as "catenated", observed in the thinner fin radials (Pazzaglia et al., 2022a, 2022b; Schaefer & Summers, 2005). These traits of the Rajiomorphii species have been extensively studied, however no definitive hypotheses, to the best of our knowledge, have been provided so far to explain the start and progression of the calcification process in the chain-like sequence of radials' columns cylindrical tiles and the relationship between calcification and longitudinal growth of the latter. In a recent study with trans-illumination and heat-deproteination techniqes, we documented the diversified calcified structure of the *Raja clavata* (Linnaeus, 1758) appendicular skeleton, suggesting a correlation with the mechanical demand (stiffening) and size/mass of the radial cartilage body (Pazzaglia et al., 2022b). Other unanswered questions concern the patterns of diversity among batoidea major lineages (Martinez et al., 2016), the phylogenetic variation of pectoral fin morphology (Franklin et al., 2014) and the systematics of the electric rays (Claeson, 2014).

This study was conducted on adult specimens of *Raja asterias*, Delaroche 1809 (Family Rajidae) and *Torpedo marmorata*, Risso 1810 (Family Torpedinidae) with a comparative morphological/morphometric approach focused on the appendicular skeleton, the correlation morphology-locomotion mechanics and the histo-morphology of the calcification process. The specific points examined in the study were: (1) 2-D and 3-D analyses of the pectoral fins dimensional geometries carried out with X-rays (1a) and trans-illumination of fin specimens after removal of skin and muscle layers (1b); (2) undecalcified and heat-deproteinated histology of the pectoral, pelvic and tail fins radials (the latter associated to sonication and lavage of of carbon combustion deposits in NaOH solutions); (3) comparison of the fin skeleton architecture between the two selected species of Rajiformes and Torpediniformes orders (3a) and among the mineralization patterns of pectoral, pelvic and tail fins in specimens of the same species but of different age (3b).

2 | MATERIALS AND METHODS

The studied adult specimens from two populations of *Raja asterias* ($n=4$) and *Torpedo marmorata* ($n=4$) were obtained from a scientific campaign in the Ligurian Sea (North-West Mediterranean) carried out by L.L. (DISTAV team, University of Genova). The work was carried out within the fishery Data Collection Framework (DCF) funded by the Italian Ministry of Agriculture, Food and Forestry policies (MIPAAF), at present MASAF (Ministry of Agriculture, Food Sovereignty and Forests), and by the European Commission (EC).

2.1 | X-rays, selection and preparation of anatomical specimens

Photos, weight and size measurements of the fishes were carried out before fixation in a solution of 10 % formaldehyde (within 12 h from the capture). X-rays in the dorso-ventral projection were taken of all the specimens. The studied skeleton regions included the whole wing disk and pelvic and tail fins of the oldest (specimens n. 4 and 8) and youngest (specimens n. 1 and 5), respectively, of *R. asterias* and *T. marmorata* (Table 1).

A careful dissection of right-wing dorsal skin, fat and muscles was carried out to obtain high-definition, dorso-ventral projection X-rays and trans-illumination images of the whole wing calcified segments. The right pectoral fin central sector with the 9 longest rays and the complete sequence of aligned radials was used for morphometry

TABLE 1 *R. asterias* and *T. marmorata* (Chondrichthyes).

n	Sex	Length (cm)	Disk-wing width (cm)	Weight (gms)	Rays number in wing (n)
Raja asterias					
1	m	29	19	123	80
2	f	30.5	21.5	179	81
3	m	40	27	343	83
4	m	52.5	34	769	80
Torpedo marmorata					
5	f	21	14	164	71
6	m	24.5	17	286	70
7	f	27	17.5	357	73
8	m	38	25	1195	72

Note: Anthropometric data of the studied populations.

(leaving only a 2 cm peripheral band of the dorsal skin covering to avoid damaging the thin outer radials).

The corresponding left-wing central sectors were separated with two full-thickness cuts and the leftover wing parts were stored in formaldehyde 4% for further histological and heat-deproteination study.

2.2 | Morphometry

The number of rays in the pectoral fins was counted on specimens X-rays (dorso-ventral projection). Microscopic morphometry was carried out on the right pectoral fin central sector of the oldest (specimen 1) and youngest (specimen 2) *R. asterias*, inferring age from the weight and size of the specimens (Table 1). The dissected sectors (after removal of skin and dorsal/ventral muscle layers) were observed unstained in trans-illumination plunged in a large Petri dish filled with a glycerol solution. The following radial parameters of the fin central sector were measured at magnification 1.25× with a stereo microscope Olympus SXZ27 using the program "Cells" (Soft Imaging System, GmbH): (1) comparative, mean radial length (distance between inter-radials joints) between sector zone **a** (radials between pterygia—duplication line) and **b** (radials distal to the last line, but excluding the band **ap**, corresponding to the 10 most apical radials); (2) the number of aligned cylindrical tiles in each column (in the zone **a** was counted only one of the diverging columns supporting the joint disk plate at the extremities). 30 radials ($n = 30$) were randomly selected in zones **a** and **b** of the central sector (Figure 3a); (3) the ratio between radial length and number of aligned tiles was used to calculate the mean tile height in each radial. The comparative, statistical analysis between the pectoral fin central sector zones **a** and **b** could be carried out only in *R. asterias* considering the pectoral fin size/shape lack of

homogeneity with of the *T. marmorata* fins. The MedCal program (MedCal Software Ltd, Ostend, Belgium) and the Student t-test was used for analysis. In all the specimens, the radials' rays most lateral band (**ap**) was not measurable due to dorsal/ventral skin superimposition. Repeated parameter measurements were obtained independently by two investigators (MR, GZ). The difference in the mean analysis (Bland & Altman, 2010) was applied to these data sets. The difference of each paired measurement (intra-observer, repeated after 30 days, and inter-observers) was plotted against observers' disagreements whose only source of variability was the measurement error. The difference of intra-observer and inter-observers data sets had a degree of agreement >95% confidence for both.

2.3 | Micro-CT

Stripes of the left wing-fins central sector corresponding to zones **a**, **b** and **ap** of the *R. asterias* oldest specimen were dissected from the skin and most of the muscles layer, dehydrated in crescent ethanol concentrated solution. These were left to dry pressed between two polyethene slides to keep them flat and to avoid curling up of the dried radials. They were then scanned with a micro-CT *XCT Research SA+* (Stratec Medizin Technik Gmbh). The files were exported from XCT in JPG format. Then the sequence was imported into *Mimics* software (Materialise) as RAW files. The resulting project was processed with a segmentation algorithm and then region growing to select areas of adjusted iso-density tissue in each section. The resulting mask was used to create a 3-D reconstruction in STL format.

2.4 | Histology and heat-deproteination

The wings of *R. asterias* (specimen 3) were split medio-laterally in segments including at least 5 radials' rays, then sectioned distinguishing zones **a**, **b** and **ap**. These specimens were dehydrated in crescent H_2O-ethanol solutions up to absolute, dried and embedded in poly-methyl-methacrylate resin. Transverse, 500 μm thick sections of each sample were sequentially cut with an IsoMet Low-speed cutter (Buehler Ltd, Lake Bluff), grinded and polished to ≈300 μm. After sonication in a bath of H_2O-ethanol solution 80 %, these were dehydrated in the alcohol series and mounted (unstained) on glass slides to be observed with an Olympus BX51 microscope (Olympus Optical Co LTD). A set of pectoral, pelvic and tail fin specimens was decalcified in a solution of acetic-hydrochloric acid (2% CH_3HCOOH/2% HCl) for two weeks, dehydrated in increasing concentrated ethanol-water solutions and embedded in paraffin. Transverse and longitudinal sections 7 μm in thickness were cut with a sledge microtome and stained with hematoxylin-eosin. Slides were observed using an Olympus BX 51 microscope (Olympus Ltd).

Dehydrated specimens of radial pectoral fin sets positioned on glass slides were subjected to heat-deproteination in a muffle

furnace at 400°C for 24h and then mounted with a cover-slip to be observed under the microscope. This technique allowed to reveal in the apical zone (**ap**) the early mineral deposition phase of the mineral deposition, which could be compared with the radials' calcified tile rows of *R. asterias* zones **a** and **b**. X-rays of *T. marmorata* caudal tail fin and *R. asterias* tail distal, dorsal fin were taken and after removal of the skin layer on one side. These were observed in trans-illumination as earlier reported for pectoral and pelvic fins.

400°C heat-deproteinated fragments of pectoral fins zone **a** radials (consisting of calcified cartilage and carbon residuals of organics combustion) were collected in a small ceramic mortar and further reduced to ≈1mm granulometry. They were repeatedly sonicated in an H_2O ethanol solution, left for 2weeks in a NaOH 0.5M solution with repeated sonications and then processed and mounted on glass slides for microscopic observation.

3 | RESULTS

3.1 | Macro-morphology, x-rays, trans-illumination and micro-CT

The *T. marmorata* outward look presents a round disk shape where the pectoral fins are not distinguishable and only dissection and X-rays allowed to characterize the inner structural layout (Figure 1a). X-rays in dorso-ventral projection highlight on the right and left sides of the spine two oval, radio-transparent soft tissue masses taking up 2/3rd of the whole disk space corresponding to the electric organs of the fish (Figure 1b,c). The pectoral fins are shifted laterally, articulating with a very wide pectoral girdle: therefore the surface area of the latter cover less than 1/rd of the disk on each side. The difference with *R. asterias* (and in general with Rajidae) is striking, because the pectoral fins of the
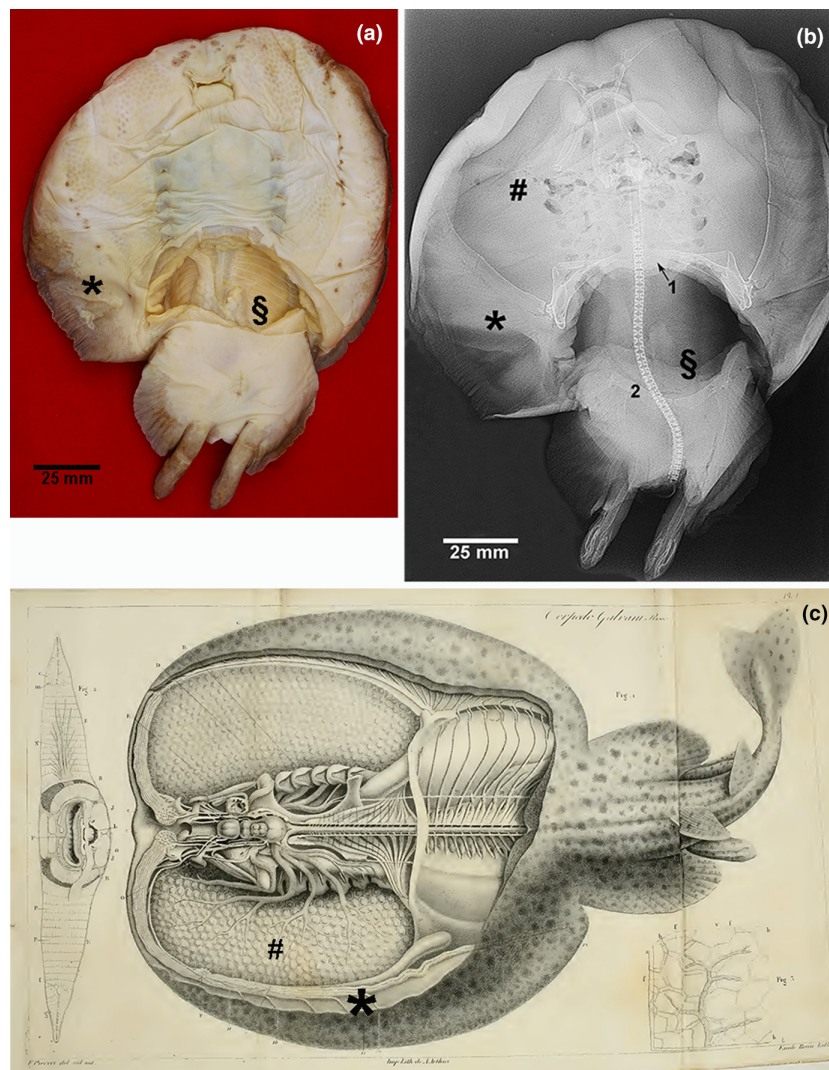

FIGURE 1 *T. marmorata*, Chondrichthyes (specimen 6, male). (a) Photograph of the ventral surface after dissection of viscera (§), showing the roundish disk shape. (b) X-rays dorso-ventral projection of the same specimen showing the large radio-transparent areas on the left and right side (#) of the spine between the pectoral fins (*). The pectoral girdle coracoid bar (1) is remarkably larger than the puboischiatic bar of pelvic girdle (2) and of the corresponding *R. asterias* structure. (c) The position of the electric organs (#) correspond to the radio-transparent spaces on both sides of the spine. (Image reproduced from Matteucci, 1844), acquired from the Donated Books Repository of the Library of Medical School, Harvard University).
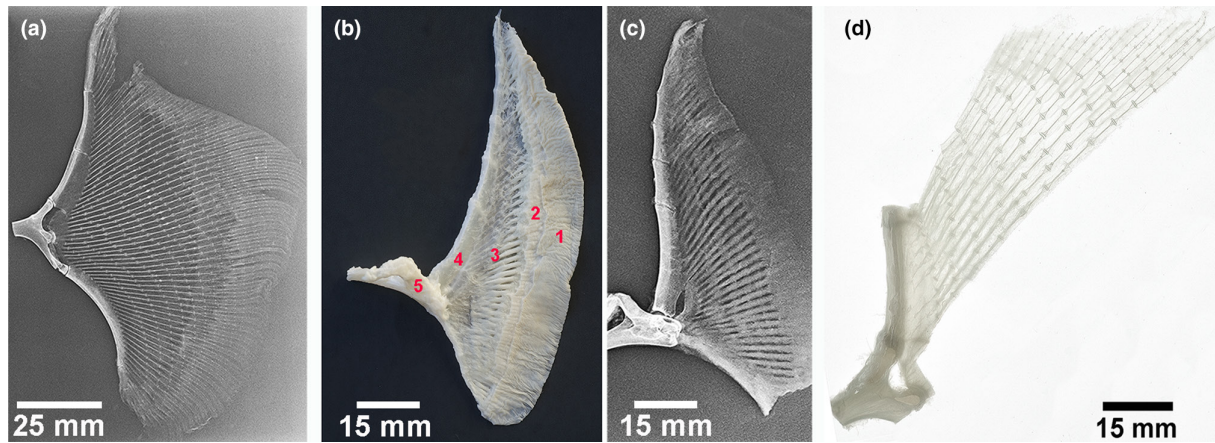
FIGURE 2 Comparison of *R. asterias* and *T. marmorata* pectoral fins. (a) *R. asterias* (specimen 4). left pectoral fin showing the lateral part of the pectoral girdle coracoid bar. The joints (diarthroses) between the latter and the pterygia and the fan of inter-radial joints forming parallel lines to the pterygia curvature. (b) *T. marmorata* (specimen 8). anatomical planes dissection of the left pectoral fin: skin (1), muscle-fascicular layer (2), calcified radials plane (3), propterygium (4) and pectoral girdle coracoid bar (5). (c) *T. marmorata* (specimen 8). macro-dissection of the fin, leaving a peripheral layer of skin to avoid damage of the most lateral radials. (d) T. marmorata (specimen 8). micro-dissection of the fin central sector documenting with trans-illumination the layout of aligned radials and joints.

latter filled the whole space of the wing (Figures 2a and 3). Comparing the two species oldest specimens, respectively n. 4 and n. 8 (Table 1), high-resolution X-rays and trans-illumination allowed to count 79 ± 04 rays in the *R. asterias* fins and 70 ± 05 in *T. marmorata* with a lower number of radials in the shorter rays of the latter. Otherwise, the fin structural texture was alike in the two species for what concerned the morphology of the inter-radial joints and the inner calcified columns of aligned tiles (Figure 3a,b). The dorso-ventral X-rays projection and trans-illumination observation showed in both species a false image of mono-columnar pattern in zone **a**, while the real layout was revealed by 3-D analysis documenting two superimposed, parallel columns (lying in the perpendicular plane of the flat wing surface). The latter were firmly linked at the radial extremities by a single joint plate which stabilized the position of the two columns (Figure 4a). At different levels of the rays (but ordered to form an arch parallel to the propterygium and metapterygium) the paired columns revolve of 90° in the horizontal plane suggesting in X-rays another false image of bifurcation (Figure 4b), but useful as reference point to distinguishing zone **a** (medial) from zone **b** (lateral). Therefore, this geometry was not correctly described by the term "duplication" because the couples of columns were already distinct in zone **a**. The true separation occurred after rotation, when each column formed its own inter-radial joint with the next lateral column, then followed by the split of the radial uncalcified body (Figure 4c) whose unquestionable evidence was provided by histological transverse sections and micro-CT (Figure 4d–g). Thereafter, the rays maintained the same mono-columnar pattern becoming progressively thinner up to the fin outer border (Figure 4g).

The smaller pelvic fins of both *R. asterias* and *T. marmorata* showed a similar layout with a series of ≈15 rays articulating laterally with pterygia of triangular shape fastened to the pelvic girdle by diarthroses (Figure 5a). The radials of the first line were up to five times longer than the more lateral segments of the same ray (Figure 5b) and of the
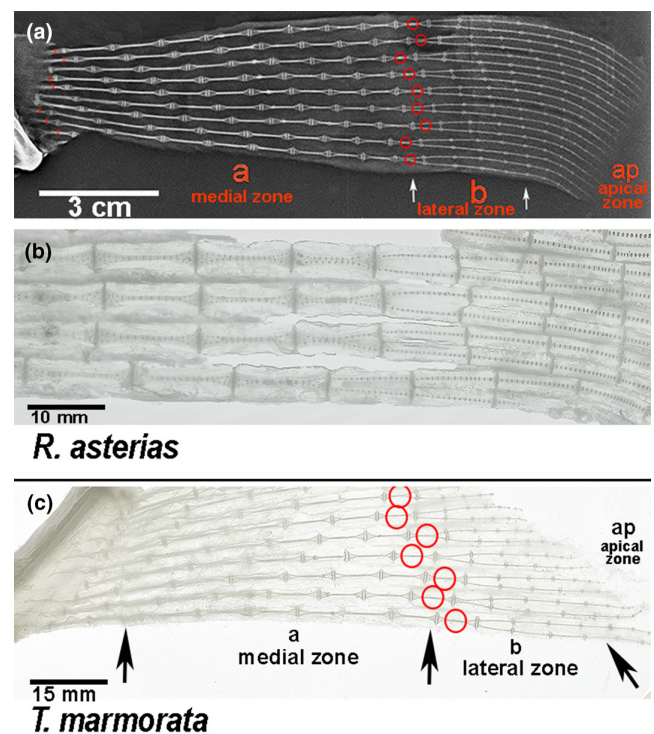
FIGURE 3 Higher-resolution comparison of *R. asterias* and *T. marmorata* pectoral fins. (a) *R. asterias* (specimen 4). X-ray of the pectoral fin central sector from pterygia to the outer border showing the radials pattern in the medial (**a**), lateral (**b**) and apical (**ap**) zone, distinguished by the duplication line of the calcified axis inside the radial cartilage body (reference points for comparative morphometry). (b) *R. asterias* (specimen 4). micro-dissected pectoral fin central sector documenting with trans-illumination the passage from zone **a** to **b** and the split of radials' uncalcified cartilage cylinders in the lateral zone. (c) *T. marmorata* (specimen 8). micro-dissected pectoral fin central sector documenting with trans-illumination the same structural pattern observed in *R. asterias* pectoral fin.
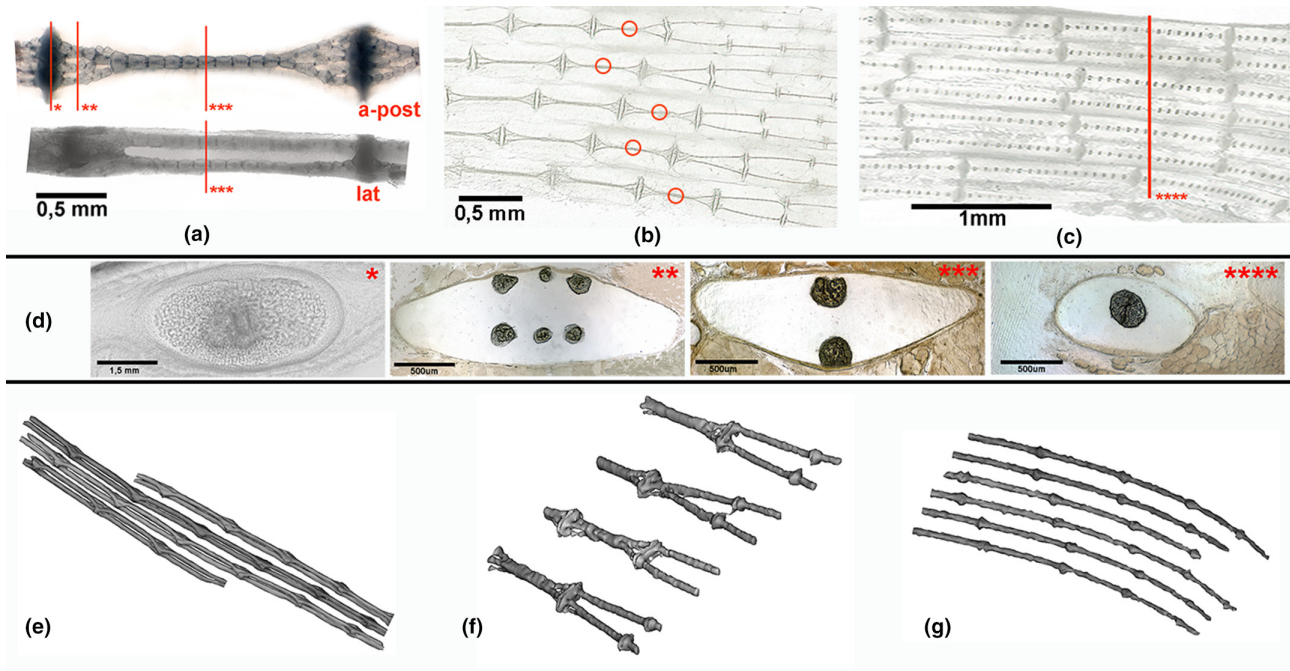
FIGURE 4 3-D analysis of zonal radials' pattern of *R. asterias* pectoral fin documenting the rotation hypothesis. (a) *R. asterias* (specimen 4). High-resolution pectoral fin zone **a** of a single radial in a-p and lateral projections (trans-illumination) showing the two parallel, calcified columns whose spatial position is kept firm by the joint disks at the radial extremities (transverse lines *, **, ***, **** correspond to transverse, histological sections of d). (b, c) *R. asterias* (specimen 4). High-resolution pectoral fin (trans-illumination) of the rotation level indicated by circles and of zone **b**, where the un-calcified cartilage cylinder was split surrounding a single column. (d) *R. asterias* (specimen 4). Transverse, undecalcified sections showing the radials' paired columns layout: * level joint disk; ** level column branching below the disk; *** level zone **a** with two columns perpendicular to the flat wing plane; **** level zone **b** with mono-columnar pattern. (c, e, f) *R. asterias* (specimen 4). Micro-CT 3-D reconstruction of radials layout respectively in zone a, transition zone and zone b.

pectoral fin radials. Their inner calcified structure was multi-columnar with a catenated tile pattern and inter-connections between the columns along the whole length (Figure 5c). The first compound radial was much bigger than the others of the same pelvic fin (Figure 5a) with a calcified texture alike that of the girdles (crustal, tesseral pattern) as formerly documented in *Raja c.f. polystigma* (Pazzaglia et al., 2022a).

An evident difference of the tail was observed between the two species: shorter, muscular and stocky in *T. marmorata*, with a caudal fin of triangular shape (Figure 6b,c), while it was long and slender in *R. asterias* and without a true terminal fin: the tail ended with a pointed extremity surmounted by the most distal dorsal fin (Figure 6d). These morpho-traits corresponded also to different calcification (Figure 6a,e) and inner structural patterns (Figure 6f) as reported in the next section 3.3 Histo-morphology.

3.2 | Pectoral fins morphometry

Trans-illumination observation under the stereo-microscope allowed to compare the radials calcified columns length, the tile number in the columns and the tiles mean height (ratio radial length/tile number). These parameters (measured in the *R. asterias* specimens 1 and 4 pectoral fin central sector) were significantly higher in zone **a** vs zone **b** of the same specimen (independently from age) as well as in the oldest vs youngest specimens, while the mean tile number was

not statistically significant (Table 2). No morphometric inter-species comparison was carried out due to the lack of pectoral fins size/shape homogeneity between *R. asterias* and *T. marmorata*. With the purpose of larger accessibility and clarity a glossary is reported (Table 3).

3.3 | Histo-morphology and Heat-deproteination

The pectoral fin radials of both species showed the same morpho-structure with elongated, hyaline cartilage bodies stiffened by single or double calcified columns of aligned tiles. At each radial top and bottom end of sector **a**, the paired tile columns spread in short branches supporting a single inter-radial joint disk (Figure 4a), while in sector **b**, the tiles at the extremities of the single columns enlarged their circumference to form the disk (Figure 4b). The passage from the sector **a** to **b** (earlier indicated in X-rays as a "duplication line") occurred when the tightly paired columns in the perpendicular plane to the flat wing surface revolved in the horizontal with a divarication of the tile columns as shown by a-p X-rays projection (Figure 4), however micro-CT transverse sections and 3D reconstruction (Figure 4e–g) provided clear evidences of the rotation, further supported by transverse sections histology (Figure 4d).

Different fin types showed variable shapes of uncalcified radial cartilage cylinder and mineralized columns: (1) oval/bi-columnar in the pectoral fins sector **a**; (2) circular/mono-columnar with central calcified tiles
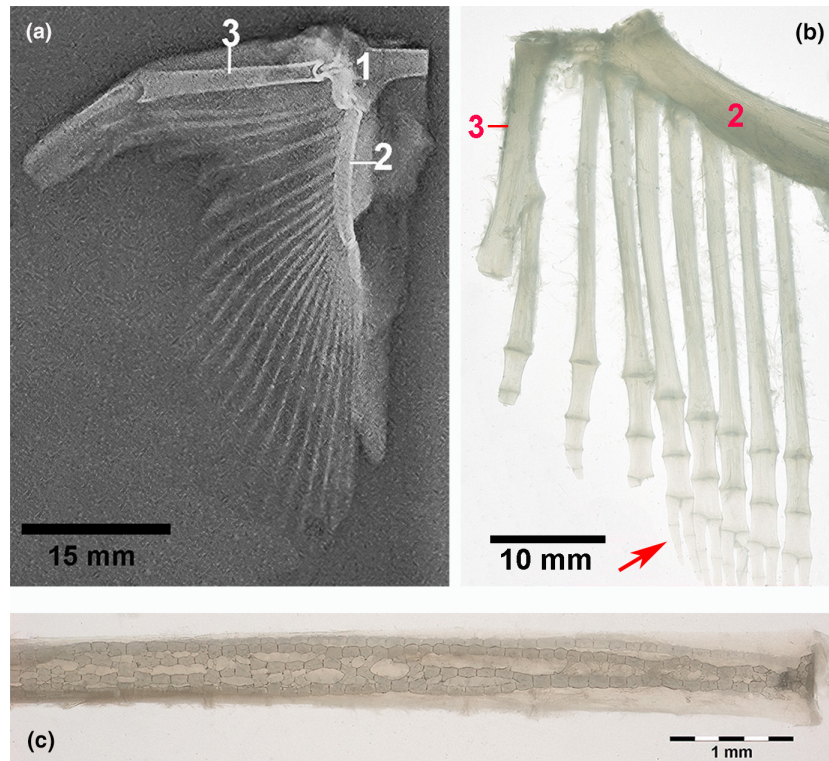
FIGURE 5 Pelvic fins X-rays and trans-illumination imaging. (a) *R. asterias* (specimen 2). X-ray of the right pelvic fin showing the lateral part of pelvic girdle puboischiatic bar (1) articulating with the compound radial through a diarthrosis, the pterygium (2) articulating laterally with a series of 21 radials. (b) *T. marmorata* (specimen 5). Trans-illumination image of dissected right pelvic fin (the diarthrosis puboischiatic bar—compound radial has been removed during dissection and the specimen is rotated 90° clockwise in respect to a). It shows: the pterygium (2) and the compound radial (3) with an anomalous joint with a radials ray. The first three most anterior rays have been cut off during dissection, the 4th—8th rays show the 1st line radials ≈ seven times the length of the more lateral segments. Bifurcation (arrow) can be observed in the most apical radials. (c) *T. marmorata* (specimen 5). High-resolution trans-illumination image of a 1st line radial documenting the inner calcified structure formed by four tiles rows with intercalating connections between single rows.

axis in sector **b** (up to the wing outer border); (3) three-cornered prismatic shaped with columns positioned at the angles and intercalary-tile connections along the ray length in the pelvic fins 1st line of segments. In the latter group, 5–6 radials were aligned along the ray length, with the first up to ten times longer than the more lateral units, the latter becoming thinner and with a short apical bifurcation. Alike in the endoskeleton tesserae, the columns' tiles calcification spread irregularly, leaving interposed, scattered areas of uncalcified matrix (Figure 7).

Trans-illumination and heat-deproteinated samples observation of the radials sequence in the rays provided evidences of the pectoral fin radials' growth pattern and calcification progression through comparison of the apical radials (zone **ap**) with corresponding medial segments of zones **b** and **a** (Figure 8). The latter technique highlighted in the apical radials a line of small calcified particles (inorganic phase) intercalated by black deposits of the burned organic phase (Figure 8c,d), while compact, larger masses of more definite cylindrical shape could be observed in the more proximal zone radials. The brown coloration was due to a diffuse inclusion of carbon deposits and higher magnification evidenced the chondrocyte lacunae contours in transparence (Figure 8c,d). The same material fragmented to ≈2–0.5 mm granulometry, repeatedly sonicated in NaOH 0.1 M solutions (then dehydrated in ethanol, dried and mounted on glass slides) displayed a felt-like texture mineralized fibers texture around chondrocytes lacunae (Figure 9a,b).

The tail fins morphology further highlighted structural differences between the two species because the *T. marmorata* fin web was supported by lepidotrichia continuous with the terminal spine segment. Unmineralized, long tapering and transparent rods (actinotrichia) expanded from the latter up to the tail outer edge (Figure 6c). The *R. asterias* tail distal, dorsal fins web showed the same actinotrichia marginal layout, however, the fin was supported by a ramification of calcified cartilage segments with the same tile pattern of pectoral fin radials (Figures 6e,f).

4 | DISCUSSION

The Batoidea appendicular skeleton essential elements are the radials which developed from the mesenchymal tissue in the embryonic and post-embryonic stages. They form a fan of rays consisting of aligned, hyaline cartilage segments with intercalated mesenchymal tissue whose cells do not undergo chondrocyte differentiation and give origin to the inter-radials joints (Maxwell et al., 2008). Therefore, the ontology of radials is not different from the "cartilage anlagen"
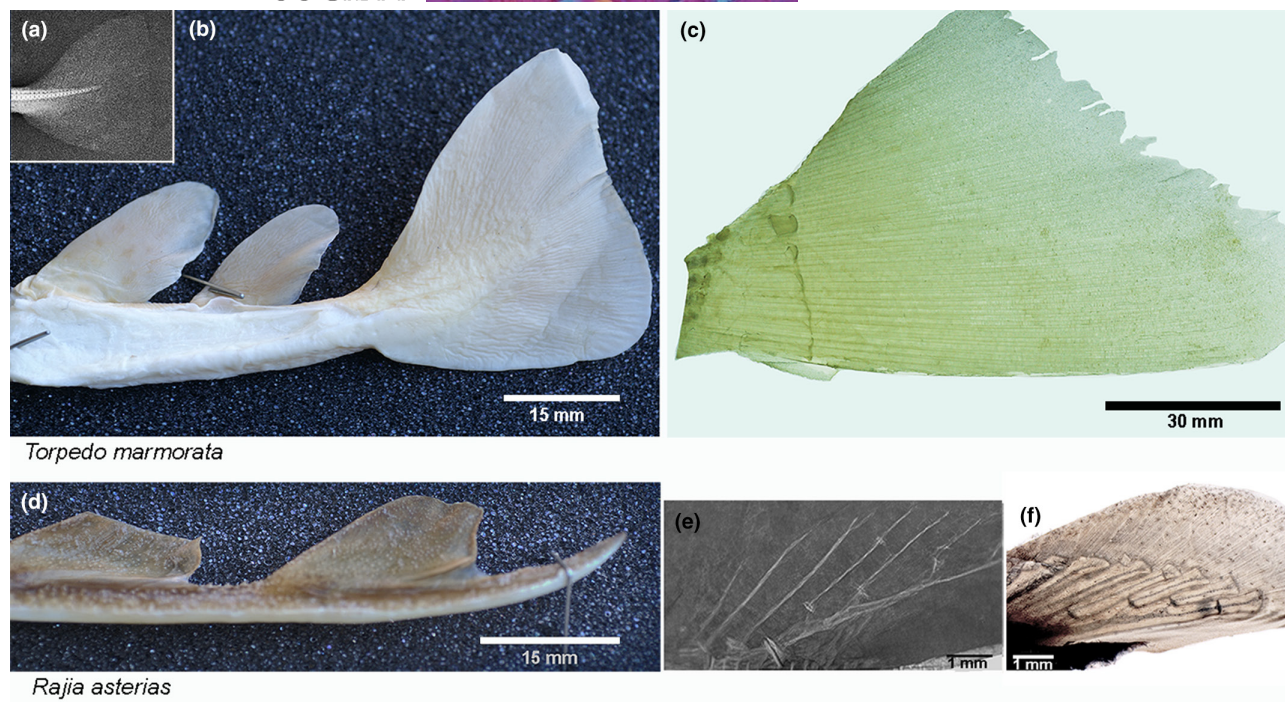
FIGURE 6 Tail fins of *T. marmorata* and *R. asterias*. (a, b) *T. marmorata* (specimen 8). Photograph and X-ray showing the stout and muscular tail ending with a bi-lobed fin (b) lacking of an inner mineralized frame (a). (c) *T. marmorata* (specimen 8). Trans-illumination of the caudal fin showing the lepidotrichia in connection with the most distal vertebrae, while long tapering and transparent rods (actinotrichia) support the fin edge. (d) *R. asterias* (Specimen 3). Photograph showing the long and slender tail ending with a pointed extremity with the placed upon most distal dorsal fin. (e, f) *R. asterias* (specimen 3). X-ray and trans-illumination image showing the calcified segments stiffening the fin (e). The latter have a radial-like structure with a central columns of tiles and expanded disks at the extremities. A fan of un-calcified actionotrichia (as in the *T. marmorata* caudal fin) spread up to the fin edge (e).

TABLE 2 *R. asterias* (Chondrichthyes).

Raja asterias							
Right wing central sector (zone a)				**Right wing central sector (zone b)**			
Specimen	**Mean rad length (μm)**	**Mean tile number (n)**	**Mean tile height[a] (μm)**	**Mean rad length (μm)**	**Mean tile number (n)**	**Mean tile height[a] (μm)**	**p**
1 *n* = 30	2335 ± 299*	20 ± 1.28^	116 ± 13°	1968 ± 158*	18.6 ± 0.77^	105.45°	**<0.001*** n.s.^ **<0.001°**
4 *n* = 30	4803 ± 525*	23 ± 1.04^	210 ± 18°	3495 ± 338*	18.1 ± 0.86^	193 ± 15°	**<0.001*** n.s.^ **<0.001°**
p	**<0.001**	n.s.	**<0.001**	**<0.001**	n.s.	**<0.001**	

Note: Comparative morphomety in wing-fin central sector (radials length and tiles number) between **a** and **b** zones and the youngest (1) and oldest (4) specimens documented no significant difference between of the calcified tiles mean number (both in the wing zone radials as well as different age specimens). These data combined with heath-deproteinated morphology of the apical radials confirmed that the tile "focal-type calcification" plays a simultaneous role with chondrocytes proliferation in the radial longitudinal growth. (The mean tile height was calculated as the ratio *mean radial length/mean tile number* and expressed as single number). Bold values indicate statistical significance of $p < 0.001$; n.s. corresponds to non-statistically significant.

[a]The tile height was calculated by the ratio rad length/tile number.

model of teleosts and other chondrichthyan fishes, birds and tetrapods (Cohn et al., 2002; Gillis, 2019; Hall, 2005, 2007) but undergoing to a different mineralization process. The growth and shaping of radials take place through chondrocyte duplication, matrix synthesis and extrusion of the latter into the pericellular space, as can be evidenced by the "cartilage anlage" size increment correlated to the density of chondrocyte mitoses, intralacunar coupled cells or paired chondrocyte lacunae (Pazzaglia et al., 2019; Pazzaglia,

**TABLE 3** Glossary of the terms used in the study.

- **Right and left wing**: (in *R. asterias*) whole anatomical structures including skin, muscles and the pectoral fin skeleton.
- **Disk**: (in *T. marmorata*) related to the round, whole fish look glanced from outside, with pectoral fin shape undistinguishable by external observation.
- **Radial**: basic unit of pectoral and pelvic fins linked at the extremities by inter-radial joints (type amphyarthroses).
- **Ray**: the sequence of aligned radials of the pectoral and pelvic fins skeleton.
- **Column**: the aligned, calcified tiles within the radial cartilage body.
- **Joint disks**: the enlarging tiles at the radial extremities forming the calcified bases of the inter-radials joint.
- **Tesserae**: calcified, polygonal units on the surface of big radials (1st compound radial), pterygia and girdle segments. These correspond to "crustal calcification".
- **Cylindrical tiles**: calcified column units. These correspond to "catenated calcification".
- **Lines**: reference to the position of radials in respect to the pterygia, so the first line is that articulating with pterygia, followed by the 2nd, 3rd, etc.
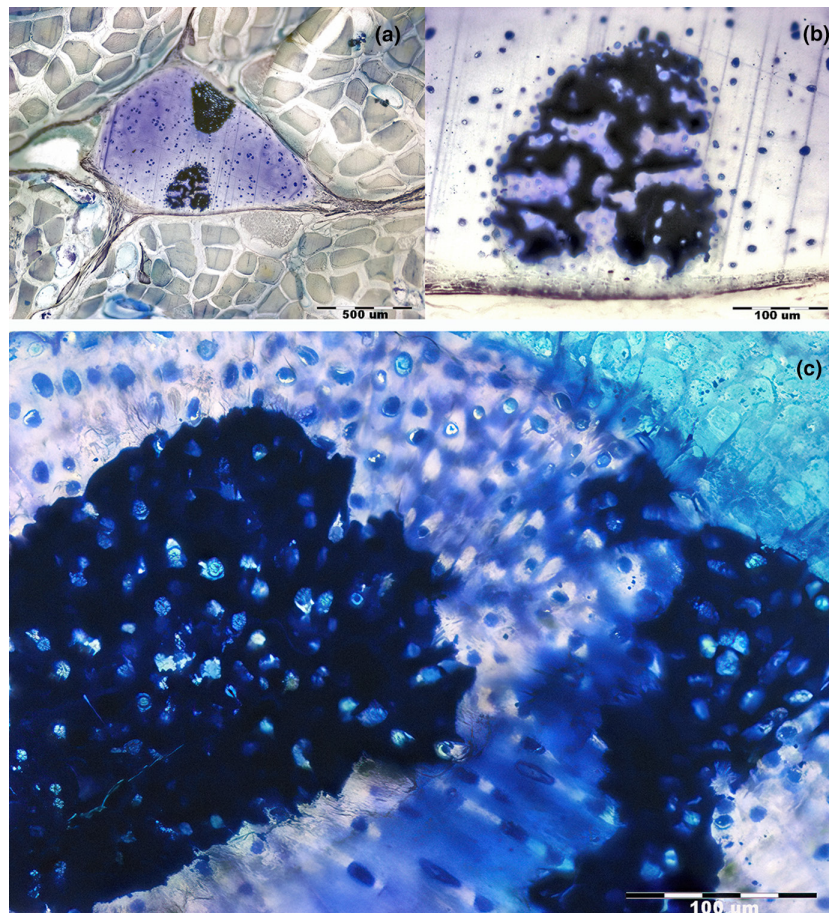
FIGURE 7 Histology of fins calcified cartilage. (a, b) (methylene-blue/acid fuchsine, 40×). Undecalcified, resin-embedded transverse section of radial bi-columnar fin. The calcified columns are placed one on another in a perpendicular plane to the flat pectoral fin surface. The upper column with a more diffuse mineral deposits, that below with scattered zones of un-calcified matrix. (c) (methylene-blue/acid fuchsine, 100×). Higher magnification documenting the scattered pattern of mineral deposition leaving interposed zones of uncalcified matrix. Chondrocytes are still evident inside lacunae of the calcified matrix. (Image reproduced from Pazzaglia et al., 2022a, Microscopic Research Technique, DOI: 10.1002/jemt.24217. Open access article distributed under the terms of the Creative Common CC, which permits unrestricted reproduction provided origin properly cited).

Congiu, et al., 2017; Pazzaglia, Reguzzoni, et al., 2017). The specific features of radials growth in the super-order Batoids (and of the Chondrictyhies in general) are correlated to a matrix mineralization process diverging from the more widespread model of endochondral ossification observable in the metaphyseal cartilage of other vertebrates (Pazzaglia et al., 2022b). The alignment and increasing volume of chondrocytes in the mammalian metaphyseal growth plate cartilages characterize the morphology of the long bones longitudinal
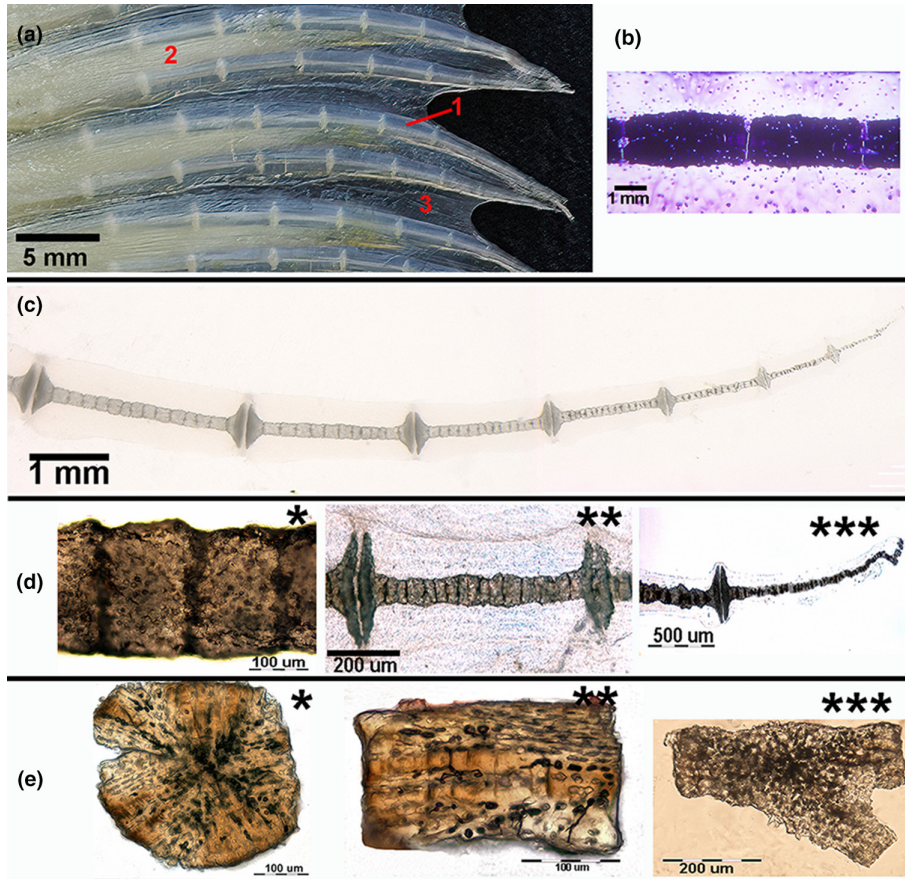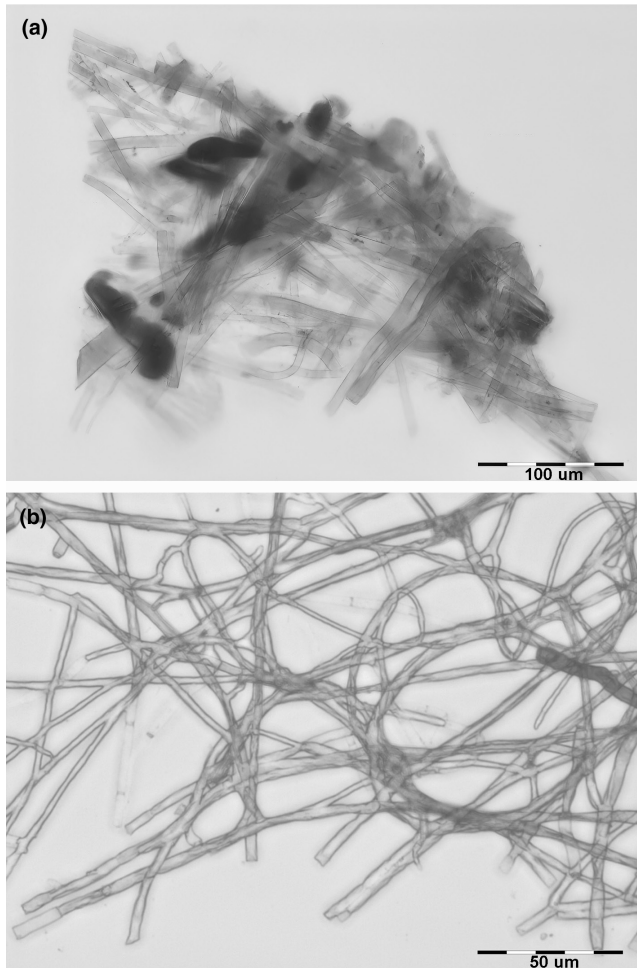
FIGURE 8 Radials growth and calcification patterns. (a) (trans-illumination image). Apical radials (sector **ap**) showing the connections between the pectoral fin rays: 1. calcified column and joint disks; 2. muscle fibers fascicles between rays. The transparent, inter-radials membrane binds the rays up to the tip. (b) (methylene-blue/acid fuchsine, 10×). Mono-culumnar radial (sector **b**) in longitudinal section, where the single, fully-mineralized tiles are still distinguishable by a thin interface (pointing out the tile as the unit of the mineral deposition process). (c) (trans-illumination image). Ray apical zone, documenting the increasing radials' length and thickness from lateral to medial. However the number of tiles (including the joint disks) remains roughly constant (≈15), supporting the assumption tile=mineralization unit. (d) (heat-deproteinated morphology). Heating at 400°C highlights the calcified cartilage phase, mixed with carbonized organic matrix (black): *column segment showing the irregular line of carbonized deposits between single tiles and within chondrocyte lacunae; ** Calcified scaffold of the whole radial with the enlarged disks at the extremities and the interposed joint spaces (amphyarthroses). The image highlights also the profile of the radial uncalcified cartilage encircling the column; *** The earlier mineral deposition is documented in the apical radials. (e) (tiles morpho-type after heat-deproteination and NaOH solution sonication). *polygonal tile (tessera) of girdles, pterygia and compound radial segments (crustal calcification); ** cylindrical tile of pectoral fin radials (catenated calcification); *** bifurcated tile of pelvic fin medial radial (interconnecting multiple columns).

growth combined with a remarkable swelling of chondrocytes which has been related to a specific mechanism of calcium and phosphate concentration mechanism leading to mineral deposition in the inter-columnar septa (Pazzaglia et al., 2020). No such ordered layout can be observed locally in the Batoids radials calcifying cartilage, even though a certain alignment of enlarged chondrocytes can be occasionally observed also in the latter. Still, the true distinguishing mark is that calcification in the metaphyseal growth plate is a provisional step providing a stiff substrate for osteoblasts apposition, later re-modeled (Pazzaglia et al., 2020), while in Batoids, the mineralized radials cartilage forms the definitive calcified units (tiles) of the skel-etal segments.

The morphometric method applied in this study through X-rays and trans-illumination allowed to measure the length of the pectoral fi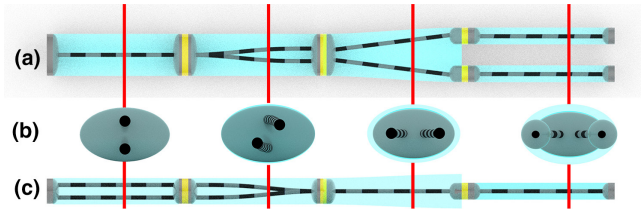n calcified columns between adjacent inter-radial joints (corresponding to the radial length). The mineral deposits morphol-ogy of the apical radials (zone **ap**) compared with that of the more medial segments in the same ray (zones **a** and **b**) suggested the un-questionable conclusion that recent mineral deposition is still occur-ing in the apical radials. No morphometric data are available from this topic literature on the uncalcified radials segmentation devel-oping in the late embryonic stage. However, the significant radials mean length differences between zone **a** and **b** of the wing central sectors suggested: (1) a simultaneous progression of the cartilage anlagen longitudinal growth and the mineralization process de-veloping within single, distinct nuclei (tiles) as documented by the not-significant difference of the radial cylindrical tiles mean num-ber between zone **a** and **b** in the same specimen and between the youngest oldest *R. asterias* specimens, and (2) a continuous growth process through the whole life cycle of the fish.

FIGURE 10 Summarizing scheme of the pectoral fins medial-lateral variable flexibility through rotation of the calcified columns within the uncalcified cartilage cylinder and split of the latter into couples of mono-columnar rays (a: dorso-ventral view; (b) transverse plane projected view; (c) lateral view).

FIGURE 9 Heat-deproteinated and NaOH solution sonicated fragments of pectoral fin radials. (a) *T. marmorata* (specimen 8). Unstained, (10×). NaOH solution removed the carbon deposits of organic matrix phase, highlighting the 3-D felt of mineralized fibers, however black combustion deposits are still evident within lacunae. (b) *T. marmorata* (specimen 8) Unstained, (400x). Detail of the loose network of calcified fibers within the fragmented tiles. This structural layout supports the hypothesis of a restricted fluid diffusion also through the elasmobranchs calcified cartilage, explaining a longer-term survival of chondrocytes embedded into the mineralized matrix of these fishes.

The pectoral and pelvic fin radials' calcified structure was alike in the two species *R. asterias* and *T. marmorata*, while the most striking differences appeared in size/shape of pectoral fins size/shape and tail caudal fins. These morpho-traits differences can be correlated with the electric organs presence in the T. marmorata wing and with the different locomotion mechanics in the water column between the two species.

The passively mobile elements (joints), the stiff segments (pterygia, radials) and the contractile effectors (muscles) form a coordinate mechanical system adapted to locomotion in the water for both the studied species and in general for the Batoidea. The stiff elements of the system are (1) the sequence of pterygia, including propterygium, mesopterygium, neopterygium and metapterygium (Compagno, 1999), the first being segmented in five parts by

amphyarthroses with practically no freedom of movement along the major axis, otherwise from the diarthrosis between the pterygia and the thoracic girdle which provide the full 3-D extension of the wing flapping movement; (2) the planar stiffness of the pectoral fin surface, modulated by the inter-radials amphyarthroses, by the flat/widespread inter-radials membrane and by the combined parameters of radial length/calcified tiles columnar structure. For what concerns the latter, the present study carried out with trans-illumination and micro-CT provided a correction of the earlier given radiographic definition of "pectoral fin radial columns bifurcation" (Pazzaglia et al., 2022b), introducing the concept of columns spatial rotation in the flat plane of the Batoids wing-fins combined with separation and autonomy of the radials in zone **b** (Figure 10). The latter represents the major structural transformation influencing the pectoral fin mechanics because it divides a stiffer medial zone from a more flexible outer part at ≈2/3rds of the whole pectoral fin wideness. The pelvic fins also showed similar graded flexibility but obtained through different structural characteristics such as the length of the 1st line radials in respect to the shorter most distal segments (length ratio ≈ 5:1) and the 1st line mono-, bi-, or multiple columnar pattern.

Experimental and descriptive studies in the species of the order Batoidea distinguished several locomotion modes: (1) undulatory and oscillatory (referred to the pectoral fins); (2) combination of axial-based/lateral-fin-based+primary thrust generated by the tail (Rosenberger, 2001); (3) punting and locomotion along the bottom (Koester & Spirito, 1999; Lucifora & Vassallo, 2002; Macesic & Summers, 2012). The significant aspects of pelvic fins shape variation have been quantified through 2-D and 3-D analysis (Blevins & Lauder, 2012; Fontanella et al., 2013), geometric morphometries (Franklin et al., 2014; Martinez et al., 2016) and swimming kinematics (Di Santo et al., 2021; Rosenblum et al., 2011) to explore the relationship of the locomotion mode with phylogeny, habitat and species behaviour. This study compared two Mediterranean species of Batoidea, focusing the attention on morphology and calcification layout, two essential elements conditioning the flexural stiffness and movement thrust efficacy developed by the wing dorsal and ventral muscles, the bilateral effectors of "flapping". Together with the diversified flexural stiffness, they characterize the mechanical system, whose kinematics has also been documented by video registrations "in vivo" during the upstroke and down stroke of the wing movement (Di Santo

et al., 2017; Rosenberger, 2001). Most of the analyses applying kinematic evidence to different Batoid species faced the problem of the wing shape variation during motion, therefore with the need to mark points on the external wing surface (thoracic fins aspect ratio) to define shape variability (Blevins & Lauder, 2012; Fontanella et al., 2013; Franklin et al., 2014; Martinez et al., 2016). Morphology and X-rays/trans-illumination imaging can be helpful to integrate data for the development of these fishes locomotion computerized models.

The pelvic fin surface area and muscular mass in both *R. asterias* and *T. marmorata* species were remarkably lower if compared with the corresponding pectoral fins, suggesting a limited relevance of the posterior fin set in the forward propulsive thrust, but with diversified actions such as turning, lateral-lateral balancing, dipping in the water column and a significant role in the dynamics linked to reproduction and the movement on the sand bottom (jumping). This study documented a reduced surface area of the *T. marmorata* pectoral fins, suggesting a lower efficiency of the "flapping effectors" than those of *R. asterias*. However, the remarkable more developed tail muscular mass of the first can compensate the lower forward thrust action with the tail oscillatory movement component. On the contrary, the *R. asterias* tail dorsal fins (stiffened by radials-like, calcified columns and few/weak muscles) rather suggested a drift-angle control mechanical function.

Batoids and Skates have been reported to use the pelvic fins' skeletal segments and the muscles of the anterior lobe to move along the bottom through repeated thrust" punting" phases (Koester & Spirito, 1999; Lucifora & Vassallo, 2002). Macesic and Summers (2012) further correlated the mineral content with the mechanical properties of pelvic pterygia (three-point bending test), reporting a flexural stiffness approaching the lower limit of other bony vertebrates segments despite 1/3rd of the mineral content in the radius-to-thickness ratio. X-rays and morphology of a recent study (Pazzaglia et al., 2022a) provided evidence of the compound radial proximal end - pelvic girdle (a socket–ball joint type) and the basipterygium—girdle (a condylar—diarthrosis type) showing below the joint sliding surface a calcified layout similar to that of mammalians. The basipterygia were segmented into four/five elements, the last ending with the clasper. At the same time, the histomorphology of the latter showed a circular layout of calcified "tesserae" like that of the pelvic girdle, matching with the calcified pattern of a vertical weight-bearing structure and with the mechanics of punting. Therefore, only the compound radial and the pterygial longitudinal axis seem to have a frame adapted to this type of stress. At the same time, no such traits are present in the pelvic fins articulating laterally with the basipterygia 1st and 3rd, 4th segments.

The cartilage calcification and the growth of Batoids endo- and appendicular skeleton poses several questions that have not been yet thoroughly answered. The scattered, apparently random topographic distribution of un-mineralized matrix areas in the skeleton calcified segments and the persistence of chondrogenesis in adult specimens has shown to develop fissures between columns of chondrocytes in the hard (calcified) zones and stretching of the collagen fibers component in the resilient uncalcified matrix (Pazzaglia et al., 2022b), while Marconi et al. (2020) correlated similar images with the presence of adult chondrogenesis and spontaneous cartilage repair. The observation of vital chondrocytes embedded inside the mineralized matrix has suggested the possibility of extra-cellular fluid exchange through a canalicular system on the model of the cortical bone network (Dean et al., 2010; Hoenig & Walsh, 1982). The heat-deproteination technique applied in this study suggested an alternative answer to the question of fluids diffusion in the Batoids calcified cartilage. The thermic treatment at 400°C burned all the matrix organic phase, while carbon residuals of combustion could be partially removed by sonication in weik NaOH solution evidencing a 3-D network of calcified fibers. Therefore, it is possible to hypothesize a fluids diffusion "in vivo" through the organic matrix phase interposed between the calcified fibers network and explaining the chondrocyte survival. The simple, experimental observation that the Batoids' endoskeleton and appendicular segments can be sectioned without difficulty with a blade, a task impossible to be carried out on calcified bone matrix, further supports the latter hypothesis. The comparative histo-morphological study between the two species *T. marmorata* and *R. asterias* documented similar structural and functional traits of the pectoral fin system but associated in the first to a remarkable reduction of the fins surface area to give space to the electric organs. On the contrary, the evolutionary plan of this species has developed a more powerful tail fins propulsive system than that of R. asterias.

CONFLICT OF INTEREST STATEMENT

None of the authors has conflict of interests.

DATA AVAILABILITY STATEMENT

The data that support the findings of this study are available from the corresponding author upon reasonable request.

ORCID

Ugo E. Pazzaglia https://orcid.org/0000-0002-3344-2388
Mario Raspanti https://orcid.org/0000-0001-6322-1845

REFERENCES

Bland, J.M. & Altman, D.G. (2010) Statistical methods for assessing agreement between two methods of clinical measurement. *International Journal of Nursing Studies*, 47, 931–936.

Blevins, E.L. & Lauder, G.V. (2012) Rajiform locomotion: three-dimensional kinematics of the pectoral fin surface during swimming

in the freshwater stingray *Potamotrygonorbignyi*. *The Journal of Experimental Biology*, 215, 3231–3241.

Claeson, K.M. (2014) The impacts of comparative anatomy of electric rays (Batoidea: Torpediniformes) on their systematic hypotheses. *Journal of Morphology*, 275, 597–612.

Cohn, M.J., Lovejoy, C.O., Wolpert, L. & Coates, M.I. (2002) Branching, segmentation and the metapterygial axis: pattern versus process in the vertebrate limb. *BioEssays*, 24, 460–465.

Compagno, L.J.V. (1973) Interrelationship of living elasmobranchs. *Zoological Journal of the Linnean Society*, 53(suppl 1), 15–81.

Compagno, L.J.V. (1977) Phyletic relationship of living sharks and rays. *American Zoologist*, 17, 303–322.

Compagno, L.J.V. (1999) Endoskeleton. In: Hamlett, W.C. (Ed.) *Sharks, skates, andrays: the biology of elasmobrancs fishes*. Baltimore: John Hopkins University Press, pp. 69–92.

Dean, M.N., Socha, J.J., Hall, B.K. & Summers, A.P. (2010) Canaliculi in the tessellated skeleton of cartilaginous fishes. *Journal of Applied Ichthyology*, 263, 263–267.

Di Santo, V., Blevins, E.L. & Lauder, G.V. (2017) Batoid locomotion: effects of speed on pectoral fin deformation in the little skate, Leucoraja erinacea. *Journal of Experimental Biology*, 220, 705–712.

Di Santo, V., Goerig, E., Wainwright, D.K. & Lauder, G.V. (2021) Covergence of undulatory swimming kinematics across a diversity of fishes. *PNAS*, 118(49), e2113206118.

Fontanella, J.E., Fish, F.E., Barchi, E.I., Campbell-Malone, R., Nichols, R.H., DiNenno, N.K. et al. (2013) Two-and three-dimensional geometries of batoids in relation to locomotion made. *Journal of Experimental Marine Biology and Ecology*, 446, 273–281.

Franklin, O., Palmer, C. & Dyke, G. (2014) Pectoral fin morphology of batoid fishes (Chondrichthyes: Batoidea): explaining phylogenetic variation with geometric morphometrics. *Journal of Morphology*, 275, 1173–1186.

Gillis, J.A. (2019) The development and evolution of cartilage. In: *Module in life sciences*. Amsterdam: Elsevier Inc. Available from: https://doi.org/10.1016/B978-0-12-809633-8.90770-2

Hall, B.K. (Ed.). (2005) Chapter 40: bones and cartilage. In: *Developmental and evolutionary skeletal biology*. San Diego, CA: Elsevier Academic Press, pp. 498–510.

Hall, B.K. (2007) *Fins into Limbs*. Chicago: University of Chicago Press.

Hoenig, J.M. & Walsh, A.H. (1982) The occurrence of cartilage canals in shark vertebrae. *Canadian Journal of Zoology*, 60, 483–485.

Koester, D.M. & Spirito, C.P. (1999) Pelvic fin locomotion in the skate, *Lecoraja erinacea. American Zoologist*, 39, 55A.

Lucifora, L.O. & Vassallo, A.J. (2002) Walking in skates (Chondrichthyes, Rajidae): anatomy, behavior and analogies to tetrapod locomotion. *J Linnean Soc*, 77, 35–41.

Macesic, L.J. & Summers, A.P. (2012) Flexural stiffness and composition of the batoid propterygium as predictors of punting ability. *The Journal of Experimental Biology*, 215, 2003–2012.

Marconi, A., Hancock-Ronemus, A. & Gillis, J.A. (2020) Adult chondrogenesis and spontaneous cartilage repair in the skate, *Leucorajaerinacea. elife*, 9, e53414.

Martinez, C.M., Rohif, F.J. & Frisk, M.G. (2016) Re-evaluation of batoid pectoral morphology reveals novel patterns of diversity among major lineages. *Journal of Morphology*, 277, 482–493.

Matteucci, C. (1844) Traite des phenomenes electro-physiologiques des animaux, suive d' etudes anatomiques sur le systéme nerveux et sur l' organe électrique de LA TORPILLE. In: White, P.D. (Ed.), *From the repositary of the library of the medical school*. Paris: Chez Fortin, Masson et Cie, Libraires.

Maxwell, E.E., Frobisch, N.B. & Heppleston, A.C. (2008) Variability and conservation in late chondrichthyan development: ontogeny of the winter skate (*Leucorajaocellata*). *The Anatomical Record*, 291, 1079–1087.

McEachran, J.D. & Dunn, K.A. (1998) Phylogenetic analysis of skates Rajidae. A morphologically conservative clade of elasmobranchs (Chondrycties: Rajidae). *Copeia*, 2, 271–290.

Pazzaglia, U.E., Congiu, T., Sibilia, V., Casati, L., Minini, A. & Benetti, A. (2017) Growth and shape of metacarpal and carpal cartilage anlagen: application of morphometry to the development of short and long bone. A study of human hand anlagen in the fetal period. *Journal of Morphology*, 278, 884–895.

Pazzaglia, U.E., Reguzzoni, M., Casati, L., Sibilia, V., Zarattini, G. & Raspanti, M. (2020) New morphological evidence of the "fate" of growth plate hypertrophic chondrocytes in the general context of endochondral ossification. *Journal of Anatomy*, 236, 305–316.

Pazzaglia, U.E., Reguzzoni, M., Manconi, R., Zecca, P.A., Zarattini, G. & Campagnolo, M. (2022a) Morphology of joints and patterns of cartilage calcification in the endoskeleton of the Batoid *Raja* cf. *polystigma. Journal of Anatomy*, 240(6), 1127–1140.

Pazzaglia, U.E., Reguzzoni, M., Manconi, R., Zecca, P.A., Zarattini, G. & Campagnolo, M. (2022b) The combined cartilage growth – calcification patterns in the wing-fins of Rajidae (Chondrichthyes): a divergent model from endochondral ossification of tetrapods. *Microscopic Research Techniques*, 85, 3642–3652. Available from: https://doi.org/10.1002/jemt

Pazzaglia, U.E., Reguzzoni, M., Pagani, F., Benetti, A. & Zarattini, G. (2017) Relationship between chondrocyte maturation cycle and the endochondral ossification in the diaphyseal and epiphyseal ossification centers. *Journal of Morphology*, 278, 1187–1198.

Pazzaglia, U.E., Reguzzoni, M., Pagani, F., Sibilia, V., Congiu, T., Salvi, A.G. et al. (2019) Study of endochondral ossification in human fetal cartilage of metacarpals: comparative morphology of mineral deposition in cartilage and in the periosteal bone matrix. *The Anatomical Record*, 301, 571–580.

Regan, C.T. (1906) Description of some new sharks in the British Museum collection. *Annals and Magazine Natural History (series 7).*, 18(65), 435–440.

Rosenberger, L.J. (2001) Pectoral fins locomotion in batoid fish's undulation versusoscillation. *The Journal of Experimental Biology*, 204, 379–394.

Rosenblum, H.G., Long, J.H. & Porter, M.E. (2011) Sink and swim: kinematicevidenceforlifting-body mechanisms in negatively buoyant electric rays Narcinebrasiliensis. *The Journal of Experimental Biology*, 214, 2935–2948.

Schaefer, J.T. & Summers, A.P. (2005) Batoid wing skeletal structure: novel morphologies, mechanical implications and phylogenetic patterns. *Journal of Morphology*, 264, 298–313.

Serena, F., Mancusi, C. & Barone, M. (Eds.). (2010) Field identification guide to the skates (Rajidae of the Mediterranean Sea). Guidelines for data collection and analysis. *Biologia Marina Mediterranea*, 17(Suppl 2), 204.

Taft, N.K. (2011) Functional implications of variation in pectoral fin ray morphology between fishes with different patterns of pectoral fin use. *Journal of Morphology*, 272, 1144–1152.